

Hybrid quantum-classical algorithms based on Semidefinite programming

Thesis submitted in partial fulfilment of the requirements
for the award of the degree of

Master of Technology

by

Sanaa Sharma

(Roll No. 19B030025)

Under the Guidance of

Prof. Himadri Shekhar Dhar



Department of Physics

INDIAN INSTITUTE OF TECHNOLOGY BOMBAY

Mumbai - 400076, India

June 26th, 2024

Thesis Approval

This thesis entitled Hybrid quantum-classical algorithms based on Semidefinite programming by Sanaa Sharma, Roll No. 19B030025, is approved for the degree of **Master of Technology**.

Digital Signature
Himadri Shekhar Dhar (10001942)
29-Jun-24 02:31:21 PM

.....

Himadri Shekhar Dhar
(Supervisor)

.....

Digital Signature
Siddhartha Santra (10001978)
01-Jul-24 09:59:21 AM

.....

Siddhartha Santra
(Examiner)

Digital Signature
Alok Shukla (i99086)
29-Jun-24 02:31:34 PM

.....

Alok Shukla
(Examiner)

Date:

Place:

Certificate

This is to certify that the thesis entitled **Hybrid quantum-classical algorithms based on semidefinite programming**, submitted by **Sanaa Sharma** to the Indian Institute of Technology Bombay, for the award of the degree of **Master of Technology**, is a record of the original, bona fide research work carried out by him under our supervision and guidance. The thesis has reached the standards fulfilling the requirements of the regulations related to the award of the degree.

The results contained in this thesis have not been submitted in part or in full to any other University or Institute for the award of any degree or diploma to the best of our knowledge.

Digital Signature Himadri Shekhar Dhar (10001942) 29-Jun-24 02:31:32 PM

.....
Himadri Shekhar Dhar

Department of Physics,
Indian Institute of Technology Bombay.

Declaration

I declare that this written submission represents my ideas in my own words. Where others' ideas and words have been included, I have adequately cited and referenced the original source. I declare that I have adhered to all principles of academic honesty and integrity and have not misrepresented or fabricated, or falsified any idea/data/-fact/source in my submission. I understand that any violation of the above will cause disciplinary action by the Institute and can also evoke penal action from the source which has thus not been properly cited or from whom proper permission has not been taken when needed.

Digital Signature Sanaa Sanaa Sharma Sharma (19b030025) 29-Jún-24 02:30:28 PM
--

Sanaa Sharma

Roll No.: 19B030025

Date:

Place: IIT Bombay

INDIAN INSTITUTE OF TECHNOLOGY BOMBAY, INDIA

CERTIFICATE OF COURSE WORK

This is to certify that Sanaa Sharma (Roll No. 19B030025) was admitted to the candidacy of M.Tech on 26th June 2023, after successfully completing all the courses required for the Master of Technology. The details of the course work done are given below.

Sl. No.	Course Code	Course Name	Credits
1	PH 575	Nanoscience: Fundamentals to Fabrication	6
2	PH 500	Thin Film Physics and Technology	6
3	PH576	Nanoscale Quantum Transport	6
4	PH 303	Supervised Learning	6
3	PH 570	Advanced Laboratory Techniques in Nanoscience	6

IIT Bombay

Date:

Dy. Registrar (Academic)

Contents

Approval

Certificate

Declaration

Certificate of Course Work

Contents

1	Introduction	1
2	Semidefinite Programming	7
2.1	Noisy Intermediate-Scale Quantum SDP Solver	9
2.2	SDP-based problems in QIS	12
2.2.1	Ground State Hamiltonian	12
2.2.1.1	Ising model-based optimization	13
2.2.2	Unambiguous State Discrimination	16
2.2.3	Lovasz Theta Number	19
2.2.4	Bell Non-locality	21
3	Ground State Energy Optimization of Molecules	23
3.1	Reduced Density Matrix Theory	24
3.2	SDP formalism of the Energy optimization problem	26
3.3	Polarized Continuum Model	27
4	Numerical Implementations of the Hybrid Algorithm	29
4.1	One-Electron Integrals	29
4.2	Mapping to the Qubit Space	32
4.2.1	PCM Optimization	34
4.2.2	Comparison with VQE calculations on Qiskit	36
4.3	Using Hadamard test in a quantum circuit	37

Contents

4.3.1	Krylov Subspace Method	39
4.3.1.1	Lanczos Method	40
4.3.1.2	The Algorithm	40

Bibliography	43
---------------------	-----------

Chapter 1

Introduction

Contemporary research in quantum computing has relied significantly on hybrid quantum-classical algorithms, which have become powerful tools for research on noisy intermediate-scale quantum (NISQ) computers ([Preskill \(2018\)](#)). Several types of hybrid algorithms, such as Variational Quantum Algorithms (VQA) ([Araújo et al. \(2023\)](#)) and Quantum Approximation Optimization Algorithms (QAOA) ([Farhi et al. \(2014\)](#)) utilize classical optimization techniques to achieve relevant solutions for a problem ([McClean et al. \(2016\)](#)). The VQA has a noteworthy property of being capable of running on any quantum device ([Peruzzo et al. \(2014\)](#)), making it a candidate for exploring the performance of early quantum computers. The algorithms are also curated in a way to make the most of present day quantum architecture.

The Variational quantum eigensolver (VQE) is hybrid, quantum classical algorithm, which means it doesn't perform all the computations on a quantum computer. A VQE takes in several different parameters, and therefore, it becomes important to choose the type of ansatz that would be employed for a particular algorithm. For a chosen set of parameters corresponding to a random state, the measurement is done and the associated energy is calculated. Subsequently, a feedback loop is

put in place that updates the parameters for a slightly changed state until a lower bound is achieved. If with each measurement, the energy gets reduced, one can say that values are converging. VQE is hybrid as the measurement (energy values) are essentially calculated on the quantum computer, while updating the parameters is done classically.

For a hybrid classical-quantum computation to be successful, two challenges need to be tackled. The first one is to choose a parameterized quantum circuit that can yield a sufficiently good approximation to the optimal solution of relevant optimization problems. While the second one depends on the classical optimization over the parameters of the quantum circuit, which will update parameters with sufficient accuracy. The classical algorithms in particular, are mostly based on gradient descent ideas ([Chen et al. \(2014\)](#)) and higher order methods ([Lovász and Schrijver \(1991\)](#)). This type of convergence is easy, as with the parameter shift rule, the gradient can be calculated efficiently.

Although VQAs can provide quantum advantage in solving different problems on near-term quantum computers, there are several challenges prominent that restricts their efficiency and accuracy. VQAs are known to be NP-hard and take an exponential time to solve ([Bittel and Kliesch \(2021\)](#)). It also suffers from non-convexity and barren-plateau problems. This makes variational optimization a rather tedious process.

One of the major problems in VQA is the barren plateau problem which refers to regions in the parameter space where the gradients of the cost function become exceedingly small, leading to slow convergence or no progress in optimization. Imagine a vast landscape with flat regions where the slope becomes nearly imperceptible. In VQAs, as the complexity of the quantum circuits increases, the parameter landscape

becomes flatter, making it difficult for optimization algorithms to find the optimal solution efficiently. To prevent the barren plateaus, researchers explore techniques like adaptive optimization methods, better initialization strategies, and introducing additional structure in the circuits to provide better guidance for efficient optimization.

The non-convexity arises due to the local minima problem 1.1. This leads to the inability of the algorithm to find the true extremum position in the solution landscape, leading to wrong results. Such problems can be tackled by using convex optimization, which offers a uniform solution landscape without the multiple minima problem.

In this report, we study hybrid quantum-classical algorithms that make use of SemiDefinite Programming (SDP), a subset of linear programming that allows for a classical optimization in NISQ algorithms. SDPs are convex optimization programs with a wide variety of applications in control theory, quantum information and computing, combinatorial optimization, and operational research. Several problems in quantum information such as quantum state discrimination ([Skrzypczyk et al. \(2019\)](#)), witnessing entanglement ([Bharti et al. \(2019\)](#)), and self-testing can be solved using SDPs ([Bancal et al. \(2015\)](#)). While SDPs can be solved conveniently in polynomial time on classical computers, high-dimensional problems may still be out of the scope of classical computers. Several methods have been devised to solve SDP efficiently in the past few decades. Even though SDPs are solvable efficiently in polynomial time on classical computers, for problems that scale exponentially with the system, quantum hardware is needed ([Bittel and Kliesch \(2021\)](#)). The polynomial runtime's description of complexity must be emphasized as being dependent on both the size of the input matrix and the number of constraints. A polynomial with an exponential degree stays exponential even when the problem's input size

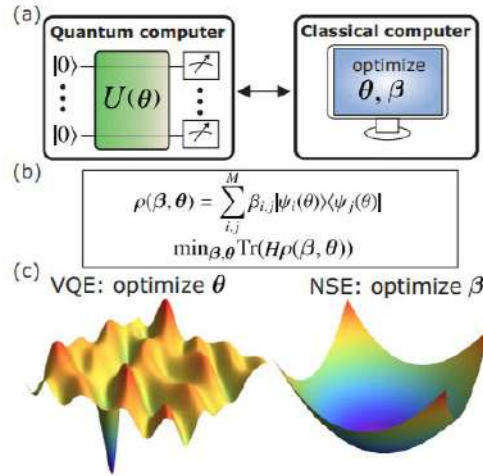


FIGURE 1.1: a) Compared to other Variational Quantum Algorithms, NSS is unique. M quantum states $|\psi_i\rangle$ are prepared and measured by a quantum computer. The hybrid density matrix, which is dependent on the combination coefficients β and the parameters θ for the parameterized quantum circuit, is optimized using a classical computer. b) The optimization job involves minimizing parameters with respect to energy $\langle H \rho(\beta, \theta) \rangle$ in order to determine the ground state of the Hamiltonian H . c) The optimization problem landscape. The variational quantum eigensolver (VQE) has a non-convex landscape, persisting far from optimal local minima, and is NP-hard when it comes to circuit parameter optimization. A semidefinite program (SDP) can solve the optimization of coefficients β in NSS in polynomial time if the optimization landscape is convex. Due to the convexity of the optimisation landscape, any local minimum is also a global minimum. (Bharti et al. (2021))

increases exponentially. As a result, typical SDPs find it difficult to handle such situations.

Our aim in this project is to make use of a general formulation to attack classically-intractable problems using a systematic use of quantum and classical resources. We exploit the quantum simulators to calculate and reduce the dimension of a problem, and then employ SDP-based post-processing techniques to optimize the results. Such a technique is needed as it not only reduces size of the problem considerably, but also allows for a convex optimization that prevents encountering issues like the barren-plateau or the local minima problem. This is done using the NISQ-SDP protocol, which will be discussed later in the report.

One of the most famous problems in quantum chemistry is that of the ground-state hamiltonian optimization. However, such studies are deeply confounded by the steep algebraic computational scaling of accurate electron correlation method, where for gold standard of electronic structure theory, namely CCSD(T), the energy values scale as N^{6-7} . Several hybrid quantum-classical algorithms have been developed to improve the computational scaling of this problem. Traditional formulations of the electronic structure problem gives rise to large linear and non-linear hermitian eigenvalue problems, however, using reduced density matrix (RDM) method, one is only required to solve a semidefinite programming problem. The SDP problem requires a positive semi-definite density matrix that maps to a density matrix (used in electronic structure theory). This density matrix describes the system without the need for a wavefunction. The SDP describes the Hamiltonian ground state issue, but this categorization does not indicate that it is an easy problem to solve ([Huang et al. \(2021\)](#)). The RDM theory gives rise to the SDP formulation and can be used to calculate optimized energy values.

In this report, we discuss a technique for mapping classically-intractable problems on quantum systems followed by a classical optimization using SDP to get results. We implement our solver on problems like the ground-state hamiltonian, lovasz theta, state discrimination as well as the solvation energy in polarized continuum model.

The main objective of the report is to study such a hybrid algorithm ([Bharti et al. \(2022\)](#)) and use the knowledge to solve several problems that can be written and optimized using SDPs. We have examined and formulated problems as SDPs and run calculations. While problems on unambiguous state discrimination, lovasz theta and the bell state problem have been explored before, we use the SDP formalism to study ground state energy optimization in detail. In doing this, we explore different hamiltonian bases and their associated energies. We also study a different type of

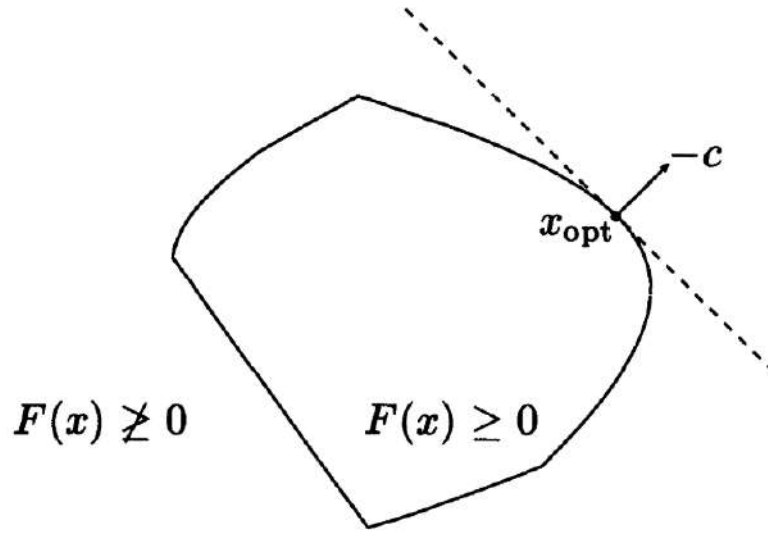
optimization using polarization matrices that calculate solvation energy in a system of solute and solvent. This system, called the Polarized Continuum Model (PCM) calculates different interaction terms using the same density matrix formalism and gives results accordingly. While the approach in most RDM theories ([Mazziotti \(2004\)](#)) require multiple matrices and constraint to achieve solutions, our method uses a general approach to achieving optimal energy solutions for a given molecule.

Chapter 2

Semidefinite Programming

In semidefinite programming, one minimizes a linear function subject to the constraint that an affine combination of symmetric matrices is positive semidefinite. Such a constraint is nonlinear and non-smooth, but convex, so semidefinite programs are convex optimization problems. Semidefinite programming unifies several standard problems (e.g., linear and quadratic programming) and finds many applications in engineering and combinatorial optimization.

Complex positive semi-definite matrices naturally appear, and have a significant role in quantum mechanics, which is effectively a linear theory in physical sciences. Therefore, several problems in the physical world can be re-written as SDPs. Such re-writing has also been rejuvenated by the advent of quantum computing and information science, which study and hope to practically perform information processing using physical objects accurately described by quantum theory ([Eldar \(2003\)](#)). Quantum information science offers an exciting opportunity to embed SDPs in optimization techniques ([Wang et al. \(2018\)](#)).

FIGURE 2.1: Simple semidefinite program with $x \in \mathbf{R}^2$, $F(x) \in \mathbf{R}^{7 \times 7}$

Although semidefinite programs are much more general than linear programs, they are not much harder to solve. Most interior-point methods for linear programming have been generalized to semidefinite programs. As in linear programming, these methods have polynomial worst-case complexity and perform very well in practice.

In semidefinite programming, we consider the problems of minimizing a linear function of a variable $x \in \mathbf{R}^m$ subject to a matrix inequality.

$$\begin{aligned} \min \quad & c^T x \\ \text{subject to} \quad & F(x) \geq 0, \\ \text{where } F(x) = & F_o + \sum_{i=1}^m x_i F_i \end{aligned}$$

Figure: 2.1 depicts a simple example with $x \in \mathbf{R}^2$ and $F_i \in \mathbf{R}^{7 \times 7}$. The boundary of the feasible region is shown as the dark curve. The feasible region, i.e., $x | F(x) \geq 0$, consists of this boundary curve along with the region it encloses. Roughly, the

semidefinite programming problems is to move as far as possible in the direction $-x$, while staying in the feasible region. For this semidefinite program, there is one optimal point, x_{opt} .

In an SDP, the non-negativity constraint $x \geq 0$ is replaced by positive semidefinite core constraint $X \succcurlyeq$. SDPs involve optimization of a linear function of matrix X over the affine slice of the cone of positive semidefinite matrices. The standard form of a SDP is given by

$$\begin{aligned} \min \quad & \text{Tr}(CX) \\ \text{subject to} \quad & \text{Tr}(A_i X) = b_i \quad \forall \quad i \in [m] \\ & X \in S_+^n \end{aligned}$$

Here, S_+^n denotes the set of $n \times n$ symmetric positive semidefinite matrices. Mathematically $X \in S_+^n | X \succcurlyeq 0$. The matrices C and A_i belong to the set of symmetric matrices S^n for $i \in [m]$. The i -th element of vector $b \in R^m$ is denoted by b_i .

2.1 Noisy Intermediate-Scale Quantum SDP Solver

The Noisy Intermediate-Scale Quantum (NISQ) SDP Solver (NSS) is a hybrid quantum-classical algorithm to solve SDPs (Bharti et al. (2021)). The NSS encodes an SDP onto a quantum computer that is integrated with an optimization routine on a classical computer. To address the scaling on the quantum side, VQE and NSE map the quantum state onto a quantum computer. Unlike the VQE which uses a parameterized initial state for calculations, the NSS uses a hybrid density

matrix. This consists of a linear combination of M -dimensional set of ansatz quantum states with classical combination coefficients β . These β values, that span a particular chosen basis, is minimized to reach the optimal energy.

The classical optimization part of the NSS is also an SDP with its dimension given by the size of the ansatz space. The NISQ SDP Solver is an attractive alternative to VQAs as it has no classical-quantum feedback loop and requires the quantum computer only for estimating the overlaps. As it has a very general approach, the NSS can be applied to a wide range of problems. The authors in the paper have described several problems, like the ground state hamiltonian, state discrimination and the lovasz theta problem, where the SDP has been used.

In comparison to VQE, the classical optimization part of the NSE can be solved in polynomial time without the local minima problem. Moreover, the SDP formalism of the solver allows user to implement various constraints in the optimization program in order to calculate excited states and solver symmetry constrained problems ([Patel et al. \(2024\)](#)).

The NISQ-SDP uses a Quantum system to create initial states and overlap integrals. The overlap integrals reduce the dimensionality of the objective SDP that is to be minimized. Next, classical optimization is carried out on a classical system. In a typical VQA, one has to feed iterated parameters back into the quantum machine as part of the feedback loop. However, this is not needed in the NISQ SDP Solver. This way, any queues to reach the quantum hardware is also avoided.

The hybrid algorithm consists of a quantum and classical optimizer. The quantum part involves generating an ansatz function and then calculating overlaps using the same functions. The overlaps reduce the dimension of the Hilbert space and hence makes it easier for the classical computer to optimize over. The classical optimization

program of the NISQ hybrid solver is another semidefinite program, but defined as an SDP over a lower dimensional ansatz space. Unlike the general VQA problem, where a quantum-classical feedback loop is used to iterate over optimization parameters, the hybrid algorithm uses Quantum measurements only once and in the beginning, specifically to create the ansatz and overlaps. The rest of the optimization is done via SDPs on classical system, This cancels the need for a feedback loop to rerun the measurements on the Quantum system. Our project revolves around understanding the algorithm used for creating the NISQ SDP solver, which can eventually be applied to general linear optimization protocols. This way, any queues to reach the quantum hardware is also avoided.

In the paper (Bharti et al. (2021)), the first step in NSS corresponds to selecting a set of quantum states $\mathcal{S} = |\psi_j\rangle \in \mathcal{H}$ over the Hilbert space \mathcal{H} , where the set contains M quantum states $|\mathcal{S}| = M$. The hybrid density matrix accordingly, takes the form

$$X_{\beta} = \sum_{(|\psi_i\rangle, |\psi_j\rangle) \in \mathcal{S} \times \mathcal{S}} \beta_{i,j} |\psi_i\rangle \langle \psi_j| ,$$

where $\beta_{i,j} \in \mathcal{C}$. It is important to understand that while the state $|\psi_i\rangle$ are prepared on quantum hardware, the $\beta_{i,j}$ terms have to be calculated classically .

For a linear problem that requires an optimal solution, one can write the operator matrices (Cost function "C" and linear constraint "A") in the selected basis as

$$D_{a,b} = \langle \psi_b | C | \psi_a \rangle$$

$$E_{a,b} = \langle \psi_b | A | \psi_a \rangle$$

These overlaps are calculated on quantum hardware using Hadamard test. Once the overlaps are calculated, it is possible to write the SDP formalism of the density matrix as

$$\begin{aligned} \min \quad & \text{Tr}(D\beta) \\ \text{subject to} \quad & \text{Tr}(E_i\beta) = b_i \quad \forall \quad i \in [m] \\ & \beta \in H_+^m \end{aligned}$$

Several examples of the NISQ-SDP hybrid SDP solvers have been discussed and analyzed in our project. Problems such as the Ground State Hamiltonian, Lovasz Theta, Largest Eigenvalue and Quantum State Discrimination have been discussed and results generated from the algorithm have been studied.

2.2 SDP-based problems in QIS

2.2.1 Ground State Hamiltonian

First, we demonstrate the NSS solver to find the ground state of Ising Hamiltonians. For implementation on quantum hardware, Hamiltonian can be written as a linear sum of unitaries such as $H = \sum_k s_k U_k$ with density matrix ρ . Therefore, the problem of finding the ground state can be written as

$$\max \quad \text{Tr}(\rho H) \tag{2.1}$$

$$\text{s.t.} \quad \text{Tr}(\rho) = 1 \tag{2.2}$$

$$\rho \succeq 0 \tag{2.3}$$

The dual formulation is:

$$\max \quad \lambda \quad (2.4)$$

$$s.t. (H - \lambda I) \succeq 1 \quad (2.5)$$

The optimum value of λ corresponds to the ground state energy. In the ansatz space generated by S , the primal SDP for the Hamiltonian ground state problem is given by

$$\min \quad \text{Tr}(\beta D) \quad (2.6)$$

$$s.t. \quad \text{Tr}(\beta) = 1 \quad (2.7)$$

$$\beta \in H_+^M \quad (2.8)$$

with $a,b = \langle \psi_a | \psi_b \rangle$ and $D_{a,b} = \sum_k s_k \langle \psi_b | U_k | \psi_a \rangle$.

The primal optimization program over β is convex and hence gives a unique minimum value. This is unlike the case of VQE, where optimization is non-convex and there can be multiple local minima. In the NSS, the classical optimization finds the optimal solution in polynomial time in the number of ansatz parameters, given that the solution is contained in the ansatz space. On the other hand, in VQAs such as VQE and QAOA, even if the optimal solution is contained in the ansatz space, the classical optimization can be NP-hard.

2.2.1.1 Ising model-based optimization

Initially, we started conducting SDP-based optimization for spin hamiltonians in order to study fermionic systems with different initial states/ ansatz. Such an optimization would allow us to study energy values without associating any physical

system to our results. This is a much simpler calculation and doesn't require molecular RDM theory implementation, giving us a chance to understand the importance of initial parameters in the method.

The Hamiltonian is described for a non-integrable Ising model of N qubits with transverse field H and longitudinal field g .

$$H_{ising} = H_z + H_x = - \sum_{n=1}^N [\sigma_{n+1}^z \sigma_n^z + g \sigma_n^z] - \sum_{n=1}^N h \sigma_n^x \quad (2.9)$$

The SDP is solved by preparing an initial state that builds up an ansatz space. There are three ways an initial space can be constructed. 1) By choosing a hardware efficient circuit $|\psi_{rand}\rangle$ constituting p -layers of randomized y -rotations and CNOT gates arranged in a chain topology, a product state $|+\rangle^{\otimes N}$ and a discretized quantum annealing state.

The algorithm uses different initial states to form ansatz functions. These states are 1) Hardware efficient circuit $|\psi_i\rangle$ comprising p layers of randomized y -rotations and CNOT gates arranged in a chain topology, 2) A product state $|+\rangle^{\otimes N}$, and 3) A discretized quantum annealing state.

The randomized quantum circuit that is used as one of our ansatz states is given by:

$$|\psi_{QA}\rangle = \prod_{k=1}^p e^{-iT \sum_{n=1}^N H_x} e^{-i \frac{Tk}{p} H_z} |+\rangle^{\otimes N} \quad (2.10)$$

where p is the number of layers of the circuit and T the quantum annealing time. The state is constructed by evolving the above equation, where we stepwise evolve with the non-commuting parts H_x and H_z . This state is a discretized form of a quantum annealing protocol, where one starts with the ground state of H_x , and

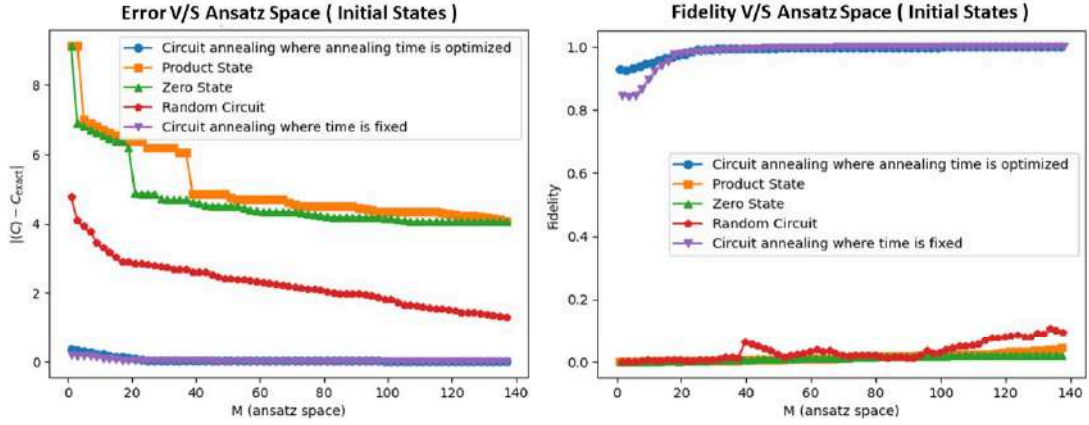


FIGURE 2.2: a) Convergence of D matrix with increasing ansatz space. D matrix is calculated as the expectation value of the Hamiltonian with optimized value of β ($\beta \langle \psi | H | \psi \rangle$). The plot shows that choice of initial states is pivotal to the convergence of the NSS. While Quantum Annealing states are the best choice for convergence, other initial state states will converge for exponentially increasing ansatz states. b) Error in overlap measurement for increasing value of M. Here (C matrix is same as D). The errors are same for Annealing states, but converge slowly for others. c) Fidelity measurements show high values for annealing states.

then slowly increases H_z until one reaches the target Hamiltonian. In the limit $p \rightarrow \inf$, the adiabatic theorem guarantees that this state becomes the exact ground state .

The results for the NISQ SDP Solver mainly depends on the initial states used to create the ansatz function (Schmidt et al. (1993)). We examine the error $\Delta E_{NSS} = E_{NSS} - E_g$ between the energy via the NSS E_{NSS} and the exact ground state energy E_g as function of M 2.2. As the size of ansatz space is increased (M), the

energy decreases and beyond a threshold M , the exact ground state is reached. The quality and accuracy of the approximation highly depends on the choice of initial state. We find that the random circuit state $|\psi_i\rangle$ converges slowly. In contrast, the quantum annealing state converges much faster to a small error and yields a good approximation of the energy even at intermediate M .

The algorithm also employs the scaling of the NSS with the number of qubits N . We use the quantum annealing state $|\psi_i\rangle$ with $p = \frac{N}{2}$ layers with energy $E_{QA} = \langle \psi_{QA} | H_{ising} | \psi_{QA} \rangle$. Now, the hybrid Q-C algorithm with initial state ψ_{QA} is applied to improve the energy estimation by using the first order of the NISQ-friendly Krylov subspace. One can observe an improvement of the NSS in estimating the energy $\Delta E_{QA}/\Delta E_{NSS}$ relative to the error of quantum annealing $\Delta E_{QA} = E_{QA} - E_g$ with increasing number of ansatz states M . The graph converges to a single curve for different number of ansatz states $M = M/3N$. The fraction improves with increasing number of ansatz M . NSS can significantly better the accuracy of finding the ground state energy even for larger number of qubits 2.3.

2.2.2 Unambiguous State Discrimination

The task of state discrimination is to identify N_S states drawn randomly from a set $G = \rho_{n=1}^{N_S}$ by performing a measurement on the state. General measurements are described by positive operator-valued measures (POVMs) $F_n \geq 0$ with the condition $\sum_n F_n = I$. If all the states are pure and pairwise orthogonal, one can simply measure with the projectors on the individual states $\Pi_n = |\psi_n\rangle \langle \psi_n|$. However, for non-orthogonal states this naive approach will result in classification errors. However, we can find a set of $N_S + 1$ POVMs that can unambiguously classify pure states. The POVMs are of the form $\sum_{n=1}^{N_S+1} F_n = I$ with $F_{N_S+1} = I - \sum_{n=1}^{N_S} F_n$. When

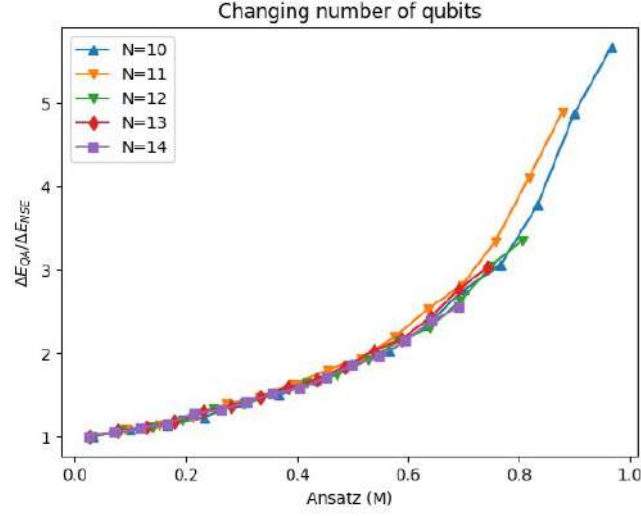


FIGURE 2.3: $\Delta E_{QA}/\Delta E_{NSS}$ for changing values N qubits. As the values of N increase, the error on the NSS increases but not very significantly. The optimization shows promise for larger systems. The graph scales equally even for larger number of qubits, which means the same solver can be applied to different systems to get equivalent results. (X axis is calculated as $\frac{M}{3N}$ state).

we measure the outcome $n \in 1, \dots, NS$ associated to POVM F_n with probability $Q_n(\rho) = \text{tr}(\rho F_n)$, we classify the measured state as ρ_n . If we measure the outcome $N_S + 1$ with POVM F_{N_S+1} , then we say that we are unable to classify the state. The problem of finding the optimal set of POVMs can be formulated as an SDP. Our goal is to optimize POVMs with respect to the average probability $Q_{correct} = 1/N_s(\sum_{n=1}^N s + 1Q_{n(\rho_n)})$ to correctly classify the states. Further, we demand that the probability of wrongly classifying state ρ_k is bounded by $Q_k^{error} = \sum_{n \neq k}^{N_s} (\rho_k F_n) \leq \epsilon$, $\forall k$ with $\epsilon \geq 0$. The SDP for NSS is formulated:

$$\max \quad \frac{1}{N_s} \sum_{n=1}^{N_s} F_n \rho_n \quad (2.11)$$

$$s.t. \quad \sum_{n \neq k}^{N_s} \rho_k F_n \leq \epsilon \quad \forall \quad k \in 1, \dots, N_s \quad (2.12)$$

$$\sum_{n=1}^{N_s+1} F_n = I \quad (2.13)$$

$$F_k \succeq 0 \quad \forall \quad k \in 1, \dots, N_s + 1 \quad (2.14)$$

$$(2.15)$$

As both the states and POVMs are constructed from the same ansatz space, we find the optimal POVMs for unambiguous state discrimination for any number of qubits. The algorithm classifies two pure states generated by a hardware efficient quantum circuit $|\psi\rangle$ which is intractable to simulate for large number of qubits. The two states ρ_1 and ρ_2 are prepared as $|\psi_k\rangle = \sum_{i,j}^M \beta_{i,j}^k P_j |\psi_{rand}\rangle \langle \psi_{rand} P_i|$ where $P_i \in S$ are a random set of M Pauli strings.

We demonstrate in Fig.5 our algorithm by classifying two pure states generated by a hardware efficient quantum circuit $|\psi_{rand}\rangle$, which is intractable to simulate for large number of qubits. The two states ρ_1 and ρ_2 are prepared as $|\psi_k\rangle = \sum_{i,j}^M \beta_{i,j}^k P_j |\psi_{rand}\rangle \langle \psi_k| P_i$ where $P_i \in S$ are a random set of M Pauli strings. The matrix E can be efficiently measured on NISQ computers. In Fig.5a, we show the probability $Q(\text{correct})$ of correctly identifying the states as function of the angle $\theta = \arccos \rho_1 \rho_2$ between the two states. We find that for demanding zero misclassification error $\epsilon = 0$, our NSS finds the analytically known optimal POVMs with $Q_{\text{optimal}} = 1 - \cos \theta$. The misclassification error refers to noise from the NISQ machines which can be represented as ϵ 2.4.

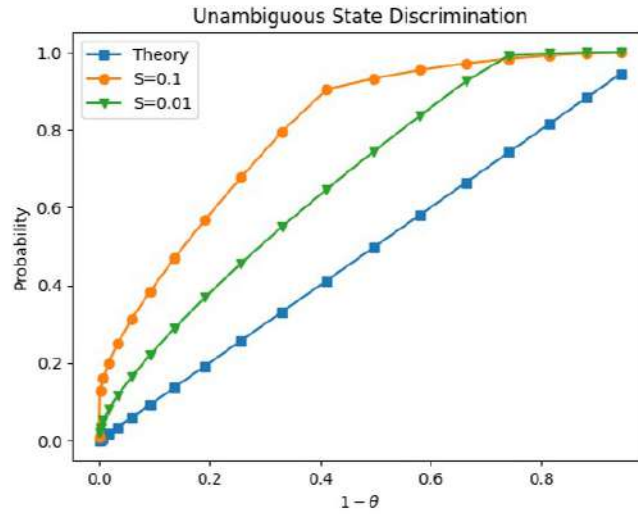


FIGURE 2.4: Unambiguous State Discrimination using our hybrid algorithm. It assumes a noise error given by ϵ and represents the variation with respect to θ which is a measure of fidelity. As the θ increases, Fidelity between two states reduces. It is easier to distinguish two states with low Fidelity, and is validated by the plot where for increases value of $1 - \theta$. Probability of correctly identifying two states increases

2.2.3 Lovasz Theta Number

Graph invariants are properties that depend only on the abstract structure of a graph. The Lovasz Theta number is such a graph invariant [Bharti et al. \(2019\)](#). The Lovasz Theta number provides an upper bound to the Shannon capacity of a graph, another graph invariant quantity. Surprisingly, it is connected with quantum contextuality and can help us to understand the potential of quantum computers ([Cabello et al. \(2014\)](#)). Given a graph $G = (V, E)$ with vertex set V and adjacency matrix E , the SDP for the Lovasz Theta number is given by

$$\max \quad JX \quad (2.16)$$

$$s.t. \quad X_{i,j} = 0 \quad \forall E_{i,j} = 1 \quad (2.17)$$

$$X = 1 \quad (2.18)$$

$$X \succeq 0 \quad (2.19)$$

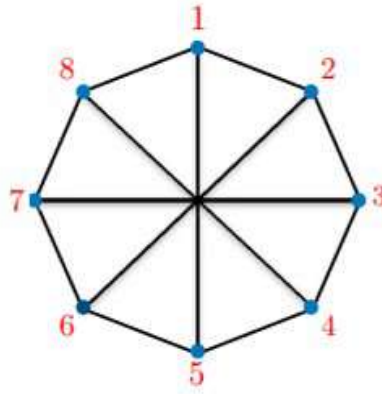


FIGURE 2.5: Graph with 8 nodes that has applications in quantum foundations and in device figure protocols. We calculate the Lovász theta number $(2 + 2)$ for this graph using NSS. (Bharti et al. (2021))

Here, J is an all one matrix. Since X is real valued, the ansatz space can be taken as real valued, which can be achieved within NSS by demanding that the ansatz quantum states are real valued. To demonstrate the NSS, we calculate the Lovasz Theta number for the graph shown in (2.5). To generate the ansatz states S , we apply a set of Pauli operators on a quantum state. We use the zero state $|0\rangle = |0\rangle^N$ or representative examples of randomized states generated via hardware efficient quantum circuits ψ_{rand} . Then, the set of basis states is generated by applying M different combinations of Pauli strings on the state $\mathbb{S} = (P_i^x |\psi\rangle)_{i=1}^M$, where $P_i^x = \otimes_{j=1}^N \sigma_j$ with $\sigma_j \in (1, \sigma^x)$.

We demonstrate the NSS's inaccuracy in the case for the Lovasz theta issue. We compute the error as the difference between the expectation values ΔC obtained from the quantum state via NSS and the exact solution $C(\text{exact})$, taking into account the problem's limitations. 2.6 As the number of ansatz states M increases, we see an improvement that culminates in the best solution when the problem's dimension is reached by the number of basis states. Depending on the initial state selected, the optimal solution can be reached with a lower number of ansatz states.

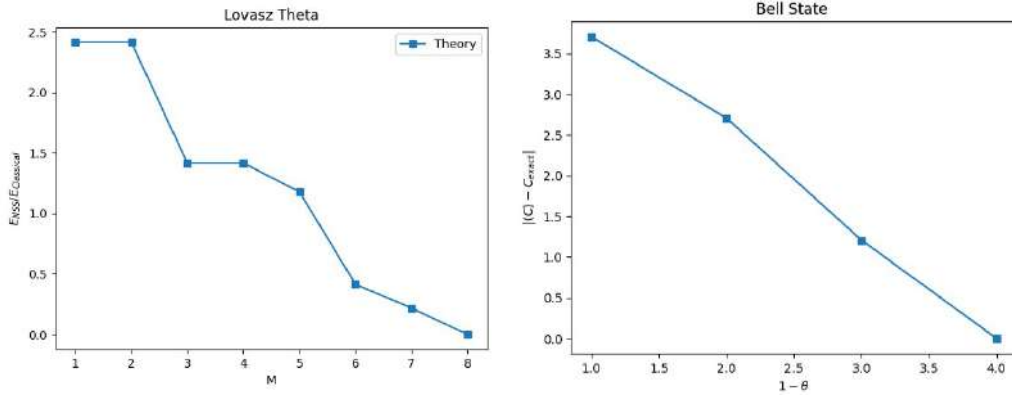


FIGURE 2.6: Error of exact solution C_{exact} and C_{NSS} plotted against number of ansatz states M . C_{exact} and C_{NSS} are vectors that contain the cost function as well as the constraints to be fulfilled. The ansatz space is generated using the all zero state $|0\rangle$. With this, we generate the M basis states $S = P_i^x \psi_{i=1}^M$, where P_i^x is one of the N -qubit Pauli strings consisting of identity I and σ_x operators. (a) NSS algorithm for Lovász theta number for the graph given in FIG with $N = 3$ qubits. (b) Bell non-local game with $N = 2$ qubits. C matrix is the vector that contain the cost function as well as the constraints to be fulfilled. The ansatz space is generated using the all zero state $|0\rangle$.

2.2.4 Bell Non-locality

The hybrid algorithm can also be used to calculate the quantum achievable success probability for the canonical Bell non-local game: the Clauser-Horn-Shimony-Holt (CHSH) game. The CHSH game involves two space-like separated parties, say, Alice and Bob. A referee asks the players uniformly random pairs of questions $x, y \in 0, 1$. The players have to answer $a, b \in 0, 1$ such that

Using the same ansatz as for the Lovász theta number, we implemented the aforementioned SDP using NSS in 2.6 and discovered that, for a sufficient number of basis states M , the proper result is obtained.

$$a \otimes b = x \wedge y \quad (2.20)$$

Here \otimes denotes addition modulo 2 and \wedge is the logical AND operator. Using classical strategies, the maximum probability of success for the CHSH game is upper bounded by 0.75. However, using quantum resources such as entangled states, the players can win the game with probability $(\cos \frac{\pi}{8})^2$. The success probability for the CHSH game can be calculated using a SDP.

Chapter 3

Ground State Energy Optimization of Molecules

The Schrodinger equation for an atom is given by

$$[\sum_{i=1}^n (\frac{-h^2}{2m} \nabla^2(\mathbf{r}) - \frac{Ze^2}{4\pi\epsilon|r_i|}) + \sum_{i<j}^n \frac{e^2}{4\pi\epsilon|r_i - r_j|}] \Psi(\mathbf{r}) = E\Psi(\mathbf{r}) \quad (3.1)$$

where m_e is the mass of an electron, and the terms account for the kinetic energy of each electron, the attractive potential between each electron and the nucleus and the repulsive potential between each pair of electrons.

The computational complexity for calculating the energy as well as the optimized wavefunction originates from the last term in the equation- the electron-electron repulsion term. For a large system, this term grows exponentially and therefore, becomes classically hard to compute. The hartree fock approximation allows us to categorize the energy terms as one-electron and two-electron terms. While the first two terms are one-electron integrals, the third term is the two-electron integral.

One can shift from the wavefunction-based approach to the RDM formulation by calculating expectation value of the hamiltonian in a certain wavefunction basis. For example, the above equation can now be translated to

$$\langle \Psi | \hat{H} | \Psi \rangle = \langle \Psi | \sum_{i=1}^n \left(\frac{-\hbar^2}{2m} \nabla^2 \psi_i^2(\mathbf{r}) - \frac{Ze^2}{4\pi\epsilon|r_i|} \right) | \Psi \rangle + \langle \Psi | \sum_{i<j}^n \frac{e^2}{4\pi\epsilon|r_i - r_j|} | \Psi \rangle \quad (3.2)$$

where the first two terms will define the one-body terms and the last term will constitute the coefficients of the two-body term.

3.1 Reduced Density Matrix Theory

Because electrons are indistinguishable with only pair-wise interactions, the energy of any atom or molecule can be expressed as a linear functional of the two-electron reduced density matrix (2-RDM). This functional allows for a variational determination of the 2RDM instead of the prevalent variation calculation of the wavefunction. The variational approach for the 2-RDM yield a lower bound on the ground-state energy in a given finite basis set. The strict lower bound occurs because the 2-RDM is optimized over a set that contains all correlated N-electron wavefunction. A practical potential of this approach is in producing ground state energies with useful accuracy even if the wavefunction is challenging to parameterize.

In quantum mechanics, the ground-state energy of any many-electron atom or molecule with Hamiltonian \hat{H} may be calculated in principle from the expectation value of the Hamiltonian with respect to the ground-state wavefunction Ψ

$$E = \langle \psi | \hat{H} | \psi \rangle$$

The molecular hamiltonian in this case is given by

$$\hat{H} = \sum_{PQ} h_{PQ} a_P^\dagger a_Q + \sum_{PQRS} g_{PQRS} a_P^\dagger a_R^\dagger a_S a_Q + h_{nuc} \quad (3.3)$$

where \hat{a}^\dagger and \hat{a} are the second-quantized creation and annihilation operators, the indices refer to the spin-orbital basis set. Here,

$$\begin{aligned} h_{PQ} &= \int \psi * _P (x) \left(-\frac{1}{2} \nabla^2 - \sum_I \frac{Z_I}{r_I} \right) \psi_Q(x) dx \\ g_{PQRS} &= \int \int \frac{\psi * _P (x_1) \psi * _R (x_2) \psi_Q(x_1) \psi_S(x_2)}{r_{12}} dx_1 dx_2 \\ h_{nuc} &= \frac{1}{2} \sum_{I \neq J} \frac{Z_I Z_J}{R_{IJ}} \end{aligned}$$

Substitution of the second-quantized Hamiltonian emphasizes the two-particle nature of the electron interaction, generating an energy expression for many-electron systems.

$$E = \sum_{i,j} {}^1K_j^i {}^1D_j^i + \sum_{i,j,k,l} {}^2K_{k,l}^{i,j} D_{k,l}^{i,j} \quad (3.4)$$

in terms of the 1-RDMs and 2-RDMs, this is written as

$$\begin{aligned} {}^2D_k^{i,j} &= \langle \Psi | \hat{a}_i^\dagger \hat{a}_j^\dagger \hat{a}_l \hat{a}_k | \Psi \rangle \\ {}^1D_j^i &= \langle \Psi | \hat{a}_i^\dagger \hat{a}_j | \Psi \rangle \end{aligned}$$

In electronic structure theory, the reduced density matrix formalism is used to reduce the dimension of large fermionic system. Moreover, density matrices of the form $\sum_{pq} \langle \psi_p | a_p^\dagger a_q | \psi_p \rangle$ are positive semi-definite and can be used in a similar kind

of optimization.

3.2 SDP formalism of the Energy optimization problem

The above equation represents an SDP formalism for matrices. The standard form of an SDP is given by

$$\begin{aligned} \min \quad & CX \\ \text{s.t.} \quad & \text{Tr}(A_i X) = b_i \quad \forall \quad i \in [m] \\ x \quad & \in \quad \mathbb{S}_+^{\times} \end{aligned}$$

Here, \mathbb{S}_+^{\times} denotes the set of $n \times n$ symmetric positive semidefinite matrices.

Mathematically speaking, $\mathbb{S}_+^{\times} := \{X \in S^m | X \succeq 0\}$. The matrices C and A_i belong to the set of symmetric matrices S^n for $i \in [m]$. The i -th element of vector $b \in R^m$ is denoted by b_i .

One can write a density matrix in a particular basis, given by

$$X_{ij} = \sum_{|\psi_i\rangle, |\psi_j\rangle \in dx} \beta_{i,j} |\psi_i\rangle \langle \psi_j|$$

where $\beta_{i,j}$ is the $d \times d$ matrix that encompasses all the basis states in the ansatz. $\sum_i^d \psi_i$ is the set of basis states used to define the density matrix X_β . An appropriate choice of states ψ_i can help reduce the dimension of the problem by presenting X_β as a reduced matrix of the same dimension as the number of basis states.

Substituting the terms for Hamiltonian (K) and density matrix D, we can write the cost function in SDP for ground-state hamiltonian problem as $Tr(HX)$. Using our reduced density matrix definition for X_{ij} , we can write the cost function as $Tr(\langle\psi_i|\hat{H}|\psi_j\rangle\beta_{ij})$. Therefore, the SDP can then be written as:

$$\begin{aligned} \min \quad & Tr(H_{ij}\beta_{i,j}) \\ \text{s.t.} \quad & Tr(\beta_{i,j}) = 1 \\ & \beta_{i,j} \in S_+^d \end{aligned}$$

3.3 Polarized Continuum Model

The Polarized Continuum Model (PCM) encompasses a physical picture of a solute embedded in a molecular shaped cavity interacting with the solvent, located outside, which is described as a structure-less polarizeable dielectric 3.1. In this approach, the charge density of the solute molecule polarizes the external environment which generates an electric field that acts back on the solute. Such a reaction field is obtained as the field produced by a set of polarization charges, the so-called apparent surface (ASC) spread on the cavity boundary whose values depend on the solute molecular electrostatic potential (MEP). In particular, implicit methods of solvation are the most commonly adopted methodology to describe the surrounding solvent as a continuum medium. Within this framework, the PCM represents a standard approach because of its flexibility and accuracy. We have used the integral equation formalism of the PCM, which allows one to describe with very little modifications to the working equations, the polarizable medium as well as the ionic solutions. We use the standard formulation of the IEF-PCM to include solvation effects in the flagship algorithms of quantum simulation for NISQ devices. The IEF-PCM approach takes

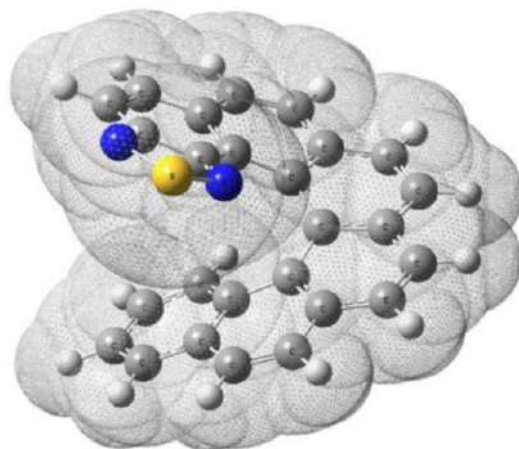


FIGURE 3.1: A molecule surrounded by solvent molecules forming a cavity. The charges on the surface of the cavity are called the Apparent Surface Charges (ASC) and interaction calculate with the Molecular Electrostatic Potential (MEP)

into account two different types of models for the solute and the solvent. While the solute molecule interactions are calculated quantum mechanically, the solvent interactions with the solute are calculated classically. The solvation energy in this case is given by:

$$\mathcal{G}[\bar{\theta}] = \sum_{p,q} h_{pq} d_{pq}(\bar{\theta}) + \frac{1}{2} \sum_{p,q,r,s} g_{pqrs} D_{pqrs}(\bar{\theta}) + \frac{1}{2} \sum_{p,q} [(j_{pq} + y_{pq}) + x_{pq}(\bar{\theta})] d_{pq}(\bar{\theta}) + \frac{1}{2} W_{NN} \quad (3.5)$$

Here p, q, r, s are indices running over the orbitals and $d_{pq}(\bar{\theta})$ and $D_{pqrs}(\bar{\theta})$ are the one and two-body RDMs. The third set of summation represents the PCM interactions (or the solute-solvent interactions) where j_{pq} is the interaction term between electrostatic potential produced by the electronic charge distribution, y_{pq} represents the interaction between the nuclear potential and the ASC generated by the elementary electronic charge distribution. Finally, x_{pq} is the interaction term between the electrons and the ASC generated by themselves.

Chapter 4

Numerical Implementations of the Hybrid Algorithm

4.1 One-Electron Integrals

The Hamiltonian of any quantum system can be written as a sum of one and two-body RDMs. For our optimization purposes, we would like to focus on the one-electron Hamiltonian and the corresponding one-RDM. The one-body terms have the most significant contribution to ground-state energy. We optimize one-electron energy values corresponding to a certain basis state chosen initially. We wish to calculate ground state energy of molecules using semidefinite programming optimization. For the initial part of our optimization, we try to calculate one-electron integrals of molecules using the molecular hamiltonian

$$H_{pq} = \Sigma_{pq} \int d^3\psi_p^*(r) \left[-\frac{\hbar^2}{2m} \nabla^2 + V(r) \right] \psi_q(r), \quad (4.1)$$

where ψ_p is the molecular orbital. H_{pq} terms for a certain basis set (in our case, it's 6-31G) are calculated using the PCM solver package.

In our initial optimization, we will take the molecular wavefunctions (i.e $|\psi_i\rangle = |\psi_p\rangle$), where ψ_p is the molecular orbital. This set of basis states spans the dimension of the problem. For example, a molecule with two molecular orbitals will have 2x1 column vector as its wavefunction.

Once the density matrix is defined in the molecular basis ψ_p , we can write it in an SDP formalism. The term \mathbf{C} in the SDP formalism is essentially the Hamiltonian H given by $\langle\psi_p|h_{pq}|\psi_q\rangle$. The β term generated from the parameter being optimized over in the SDP.

$$\begin{aligned} \min \quad & Tr(H_{pq}\beta_{pq}) \\ \text{s.t.} \quad & Tr(A\beta_{pq}) = 1 \\ & \beta_{pq} \in S_+^d \end{aligned}$$

Here, d is the same dimension as the Hamiltonian (H_{pq}). The matrix \mathbf{A} defines the set of linear constraints on β_{pq} . In this case, $\beta_{p,q}$ becomes the reduced density matrix, and the SDP problem is essentially minimizing its trace with respect to the constraint that the trace of this term is 1 and that it is positive semi-definite.

We begin with the SDP optimization of Hamiltonians in the MO basis and calculate one-electron energies for H_2 , H_2O , HeH^+ and H_3O^+ . We get the hamiltonian form Psi4 calculations and associated one-electron terms. For these terms, we calculate the β matrix, which is also the RDM in this case. The results are shown in Figure:4.2. Both the SCF and the SDP energies are calculated in the 6-31G basis and the SDP energy curves adopt a similar path as the SCF values.4.1

The energy in 4.1 shows the close behavior of the SDP optimization of the one-electron hamiltonians with the actual 6-31G energies. It is important to note that we have only tried to minimize the one-electron terms here as the two-electron interaction is a larger matrix. Both the matrices cannot be optimized together but individually, one can calculate the minimum energies.

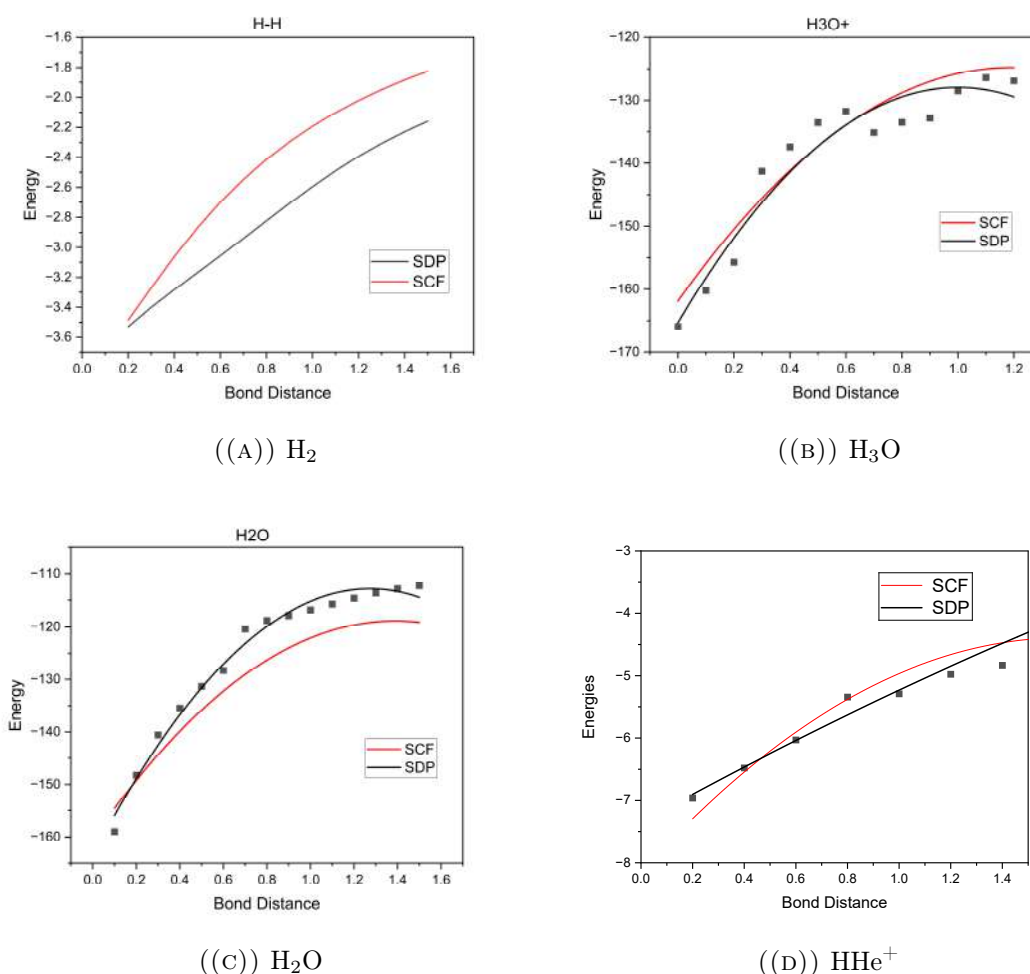


FIGURE 4.1: Energy difference between SCF and SDP optimization in the qubit basis set. Here the molecules are a) H_2 , b) H_3O^+ , c) H_2O , d) HHe^+ .

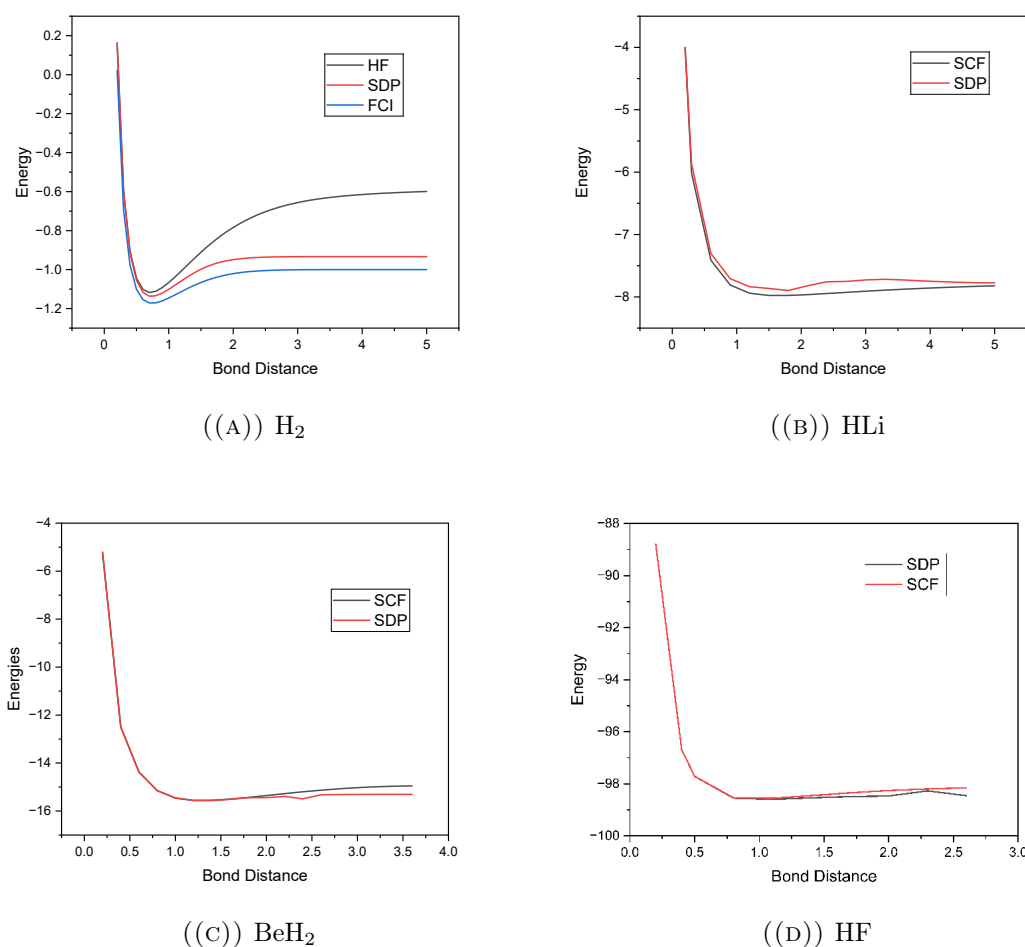


FIGURE 4.2: Energy difference between SCF and SDP optimization in the qubit basis set. Here the molecules are a) H_2 , b) HLi , c) BeH_2 , d) HF .

4.2 Mapping to the Qubit Space

The application of accurate classical methods are severely limited by the fast growing computational cost, therefore, quantum computation is essential to solve such problems in chemistry. By encoding the wavefunctions into the Hilbert space of qubits, the Schrodinger equation for molecular systems can be solved on a quantum computer. Such encoding techniques are common in variational quantum algorithms.

An important concept to understand the molecular basis to qubit basis mapping is

of the Fock space. Let $\psi_P(\mathbf{x})$ be a basis of M orthonormal spin orbital, where the coordinate \mathbf{x} represent collectively the spatial coordinator and the spin coordinates σ of the electron. A Slater determinant is an anti-symmetrized product of one or more spin orbitals. For example, a normalized Slater determinant for N electrons can be written as

$$|\psi_{P_1} \dots \psi_{P_N}\rangle = \frac{1}{\sqrt{N!}} \begin{vmatrix} \psi_{P_1}(x_1) & \dots & \psi_{P_N}(x_1) \\ \dots & \dots & \dots \\ \psi_{P_1}(x_N) & \dots & \psi_{P_N}(x_N) \end{vmatrix}$$

We now describe an abstract linear vector space- the Fock space- where each determinant is represented by an occupation-number (ON) vector $|\mathbf{k}\rangle$.

$$|k\rangle = |k_1, k_2, \dots, k_M\rangle, k_P = \begin{cases} 1, & \psi_P \text{ occupied} \\ 0, & \psi_P \text{ unoccupied} \end{cases} \quad (4.2)$$

Thus the occupation number k_P is 1 if ψ_P is present in the determinant and 0 if it is absent. For an orthonormal set of spin orbitals, we define the inner product between two ON vectors $|k\rangle$ and $|m\rangle$ as

$$\langle k|m\rangle = \delta_{k,m} = \prod_{P=1}^M \delta_{k_P m_P} \quad (4.3)$$

This definition is consistent with the overlap between two Slater determinants containing the same number of electrons.

To simulate a system of fermions on a quantum computer, we must choose a representation of the ladder operators on the Hilbert space of the qubits. In other words,

we must designate a set of qubit operators (matrices) which satisfy the canonical anticommutation relations. Qubit operators are written in terms of X, Y and Z Pauli matrices. Moreover, we also need to write our wavefunctions in the occupation number basis, which can directly be mapped to the qubit basis.

For example, Hydrogen molecule, we start with two molecular orbitals that can be mapped to four spatial orbitals. Once this is done, we have an occupation vector of 4 terms that describe the presence of a fermion in that particular orbital. A typical ground state wavefunction will translate to $|1100\rangle$ vector, where the first two spatial orbitals are occupied in the ground state.

Mapping to a qubit space from the molecular basis results in increasing the dimension of the problem exponentially (2^N), giving rise to very large matrices when solving bigger molecules. An STO-3G hamiltonian for H₂ is 2x2 matrix, while the same hamiltonian when mapped to a qubit operator using the famous Jordan Wigner mapping gives a 16x16 hamiltonian. [4.2](#)

4.2.1 PCM Optimization

We refer to ([Castaldo et al. \(2022\)](#)) paper to incorporate new applications of our approach in calculating optimal energies. The polarized energies can be calculated by writing the polarization matrices separately. This hamiltonian is solved with a certain density matrix like in our previous calculations. In our calculations, we use the Psi4 PCM Solver package to get the Hamiltonians and the wavefunctions. The polarization matrices according to this PCM model with DMSO₄ as the solvent are then calculated.

The PCM solver uses the IEF-PCM method to calculate energies. In this particular solver, the interactions of the solute molecule are quantum mechanically, while

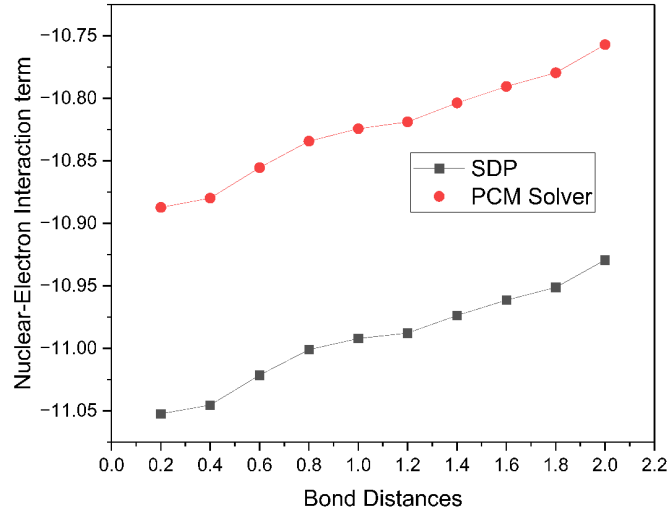


FIGURE 4.3: PCM V/S SDP energy for the $j_{pq} + x_{pq}$ matrices of water molecule with DMSO solvent

the solvent interactions are classically approximated. The solute-solvent interaction surface is defined as a cavity with small area divisions known as the tesserae. Each tesserae in the cavity has different Apparent Surface Charge (ASC), and is used to calculate the interaction between the Molecular Electrostatic Potential (MEP) and the solvent outside.

$$H_{PCM} = \frac{1}{2} \sum_{p,q} [(j_{pq} + y_{pq}) + x_{pq}(\bar{\theta})] d_{pq}(\bar{\theta}) \quad (4.4)$$

The terms j_{pq} here correspond to the interaction term between electrostatic potential produced by the electronic charge distribution and the ASC generated by the nuclear charge distribution. Similarly, y_{pq} represents the interaction between the nuclear potential and the ASC generated by the elementary electronic charge distribution. Finally, x_{pq} is the interaction term between the electrons and the ASC generated by themselves.

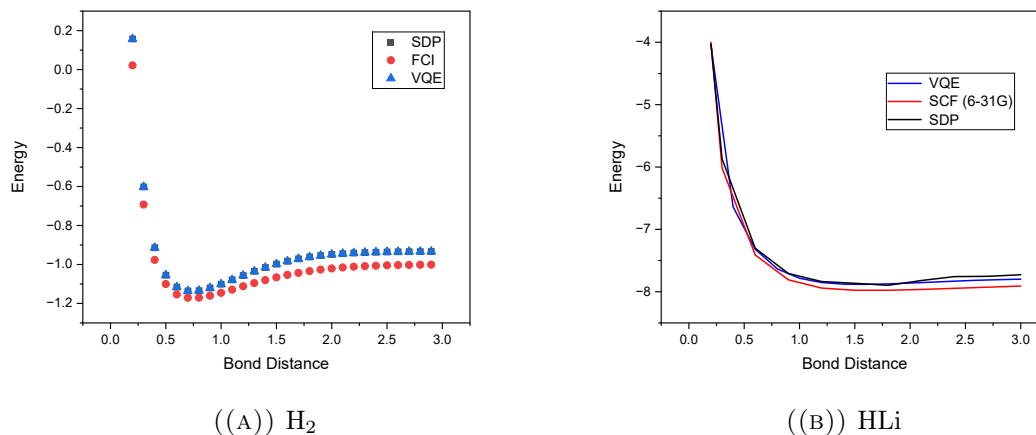


FIGURE 4.4: Energy comparison for H_2 and HLi molecule. Qiskit VQE energies are same as the ones calculated using SDP to the fourth order in H_2 . The SDP solver gives accurate results close to the exact terms for both the molecules

Figure 4.4 describes the interaction energies between the ASC of the solvent and the nuclear energy of the solute for H_2O molecule. These terms are calculated for the all tessera and the energies accordingly calculated. Both the calculations are done in the STO-3G, which is the minimal basis set. We see that the energy terms are close and almost follow the same pattern/behavior.

4.2.2 Comparison with VQE calculations on Qiskit

To ascertain the accuracy of our approach to the conventional Qiskit VQE application, we compare the energy values of H_2 calculated using VQE as well as through SDP. The values are given in the table below 4.2.2. The energies are very similar and therefore, the plot 4.4 doesn't show SDP values.

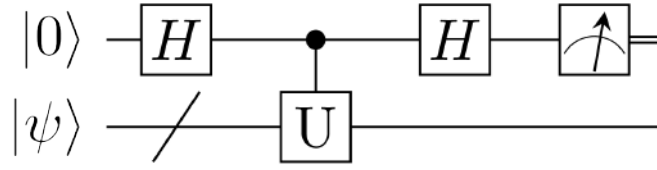


FIGURE 4.5: Circuit used for Hadamard test

Bond Distance	SDP	VQE
0.5	-1.055177087	-1.05516
0.6	-1.11628283	-1.11629
0.7	-1.136176472	-1.13619
0.8	-1.134149835	-1.13415
0.9	-1.120563794	-1.12056
1.0	-1.101145551	-1.10115
1.1	-1.079221122	-1.07919
1.2	-1.056740751	-1.05674
1.3	-1.035200343	-1.03519
1.4	-1.015468252	-1.01547

4.3 Using Hadamard test in a quantum circuit

The overlaps $H_{pq} = \langle \psi_p | H_{pq} | \psi_q \rangle$ can be measured using the Hadamard test. In quantum computation, the Hadamard test is a method to calculate overlaps ($\langle \Psi | U | \Psi \rangle$) where $|\Psi\rangle$ is a quantum state and U is the unitary gate acting on the space of $|\Psi\rangle$. The Hadamard test produces a random variable whose image is in $\{\pm 1\}$ and whose expected values is $\langle \Psi | U | \Psi \rangle$. Figure 4.5 shows the circuit required to calculate overlaps using the Hadamard test. Here, we look at the NISQ SDP Solver implementation of the above mentioned optimization. We begin by calculating the

terms $\langle \psi_p | H_{pq} | \psi_q \rangle$. First, we retrieve the H_{pq} term from PCM solver package for H_2 molecule. This term, H_{pq} is then decomposed into sum of unitaries (pauli strings) that implementable on a quantum circuit: $H = \sum_k s_k U_k$. The algorithm for the Hadamard test is explained below:

- Initialize: $|0\rangle$ (ancilla) and $|\psi\rangle$ (system)
- Hadamard Gate on Ancilla

$$H |0\rangle = \frac{1}{\sqrt{2}}(|0\rangle + |1\rangle) \quad (4.5)$$

- Controlled-U gate:

$$\frac{1}{\sqrt{2}}(|0\rangle \otimes |\psi\rangle + |1\rangle \otimes U |\psi\rangle) \quad (4.6)$$

- Hadamard Gate on Ancilla:

$$\frac{1}{2}(|0\rangle \otimes (|\psi\rangle + U\psi) + |1\rangle \otimes (|\psi\rangle - U |\psi\rangle)) \quad (4.7)$$

- Measure Ancilla: Calculate probabilities and estimate $Re(\langle \psi | U | \psi \rangle)$

$|\psi_p\rangle$ and $|\psi_q\rangle$ are written as occupation number vectors. For hydrogen, we take 4 qubits for four different spin orbitals. Therefore, the dimension of the occupation vector is 16x1. Similarly, the hamiltonian is also a 16x16 matrix. Occupation vectors ψ_p and ψ_q are given as $|0011\rangle$ and $|1100\rangle$.

The following is the result for hydrogen atom ground state energy calculated using the Hadamard test 4.6.

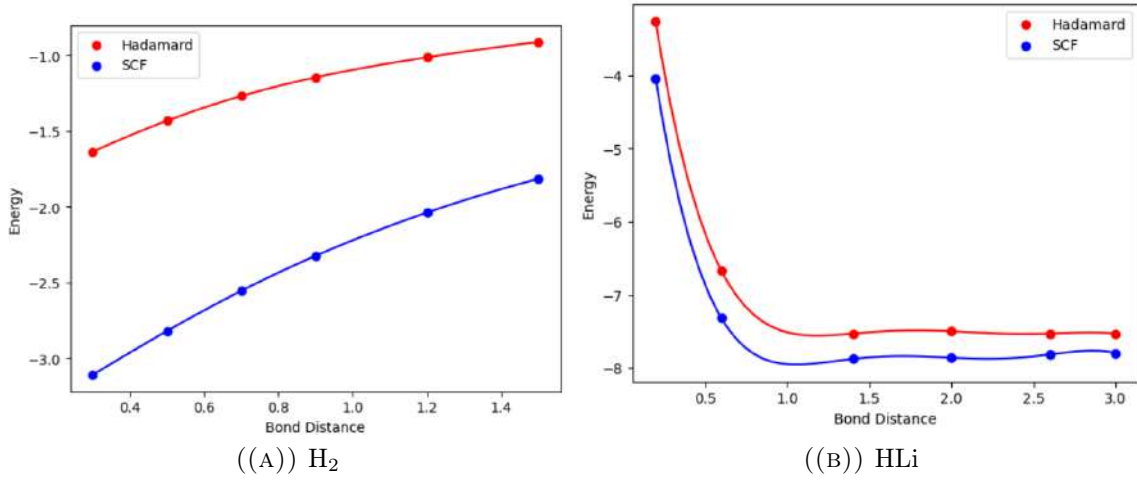


FIGURE 4.6: Energy values on increasing bond distance in H₂ and HLi. We see the SDP results following a similar trend as that for SCF optimization with 6-31G basis. This serves as a proof-of-concept of implementing energy calculations on quantum circuit using our SDP-based approach.

Using the figure 4.5, we calculate the energies of H₂ molecule for a minimal occupation vector spanning 4 qubits. The occupation vectors, or the ansatz, is given by $|1100\rangle$ and $|0011\rangle$, resulting in a 16X1 column vector that represents four spatial orbitals in H₂. We now use the 2 occupation vectors to calculate 4 terms, i.e., $\langle\psi_i|H|\psi_j\rangle$. These terms make a 2x2 matrix. In Qiskit, we begin by first creating our initial states, and then writing the hamiltonians as a linear combination of different unitaries (pauli matrices). For a set of 100 shots, we calculate the expectation values for every Pauli string in the decomposition. The more the number of shots, better is the accuracy of the results. In 4.6, we show the results for a small system of H₂

4.3.1 Krylov Subspace Method

The krylov subspace is a sequence of subspaces generated by repeatedly applying a matrix to a vector. Formally, for a given $n \times n$ matrix H and an initial vector v , the

m-th Krylov subspace is defined as:

$$K_m(H, v) = \text{span}\{v, Hv, H^2v, \dots, H^{m-1}v\} \quad (4.8)$$

where:

- v is the initial vector (the random vector)
- H is the matrix for which we are generating the Krylov subspace
- m is the dimension of the subspace

The vectors $v, Hv, \dots, H^{m-1}v$ are linearly dependent when m exceeds the dimension of the matrix H . The krylov subspace is used in iteracitve methods for solving linear systems and eigenvalue problems because it captures the action of the matrix H on the space spanned by the initial vector.

4.3.1.1 Lanczos Method

The Lanczos method is an iterative algorithm used to reduce a large Hermitian (or symmetric) matrix H to a tridiagonal form T . This is particularly useful for finding the eigenvalues and eigenvectors of H . The method constructs an orthonormal basis from the Krylov subspace using the Lanczos process and generates a sequence of orthogonal vectors.

4.3.1.2 The Algorithm

Given an $n \times n$ Hermitian matrix H and an initial vector v_0 , with $\|v_0\| = 1$, the Lanczos algorithm proceeds as follows:

- Initialization: Set $v_1 = v_0$
- Iteration (for $j=1$ to m):
 - Compute $w_j = Hv_j - \beta_{j-1}v_{j-1}$
 - Computer $\alpha_j = v_j * w_j$
 - Update $w_j = w_j - \alpha_j v_j$
 - Orthogonalize w_j against the previous vectors to maintain orthogonality
 - * $w_j = w_j - \sum_{i=0}^{j-1} (v_i * w_j) v_i$
 - Compute $\beta_j = ||w_j||$
 - Normalize $v_{j+1} = w_j/\beta_j$
- Construct the tridiagonal matrix T
 - The tridiagonal matrix T has the diagonal elements α_j and off-diagonal elements β_j

In our case, we intend to do a full renormalization of the vectors using Gram-Schmidt Decomposition and study the results of molecular hamiltonians with reduced dimensions.

We employ the algorithm to benchmark the quality of our results with the actual eigenvalues of the matrix. To calculate the eigenvalues of the large matrix \mathbf{H} , we use Scipy's "eigsh" sparse solver to get the smaller eigenvalues. On the other hand, the energy of the reduced hamiltonian is calculated via the "linalg.eigh" function. Table 4.3.1.2 refers to the energies calculated and their difference.

Matrix Dimension	Sparse Solver	SDP+Krylov	Difference
1000	-128.2098756	-128.1418157	0.06805989
2000	-182.3238906	-182.051643	0.272
3000	-222.1781658	-222.22176	0.0436
4000	-256.839428	-256.688528	0.151
5000	-287.9160533	-288.1418814	0.22582807

Such a method can be employed to reduce the dimension of molecular hamiltonians, which grow exponentially with the size of the system. Once the size of the system is reduced, the smaller hamiltonian can be solved using our SDP formalism. Such an approximation holds promise in case of very large molecules for which VQE and other quantum methods fail to give the correct results.

References

- Araújo, M., Huber, M., Navascués, M., Pivoluska, M., Tavakoli, A., 2023. Quantum key distribution rates from semidefinite programming. *Quantum* 7, 1019. URL: <https://doi.org/10.22331/q-2023-05-24-1019>, doi:10.22331/q-2023-05-24-1019.
- Bancal, J.D., Navascués, M., Scarani, V., Vértesi, T., Yang, T.H., 2015. Physical characterization of quantum devices from nonlocal correlations. *Phys. Rev. A* 91, 022115. URL: <https://link.aps.org/doi/10.1103/PhysRevA.91.022115>, doi:10.1103/PhysRevA.91.022115.
- Bharti, K., Haug, T., Vedral, V., Kwek, L.C., 2021. Nisq algorithm for semidefinite programming. arXiv preprint arXiv:2106.03891 .
- Bharti, K., Haug, T., Vedral, V., Kwek, L.C., 2022. Noisy intermediate-scale quantum algorithm for semidefinite programming. *Phys. Rev. A* 105, 052445. URL: <https://link.aps.org/doi/10.1103/PhysRevA.105.052445>, doi:10.1103/PhysRevA.105.052445.
- Bharti, K., Ray, M., Varvitsiotis, A., Warsi, N.A., Cabello, A., Kwek, L.C., 2019. Robust self-testing of quantum systems via noncontextuality inequalities. *Phys. Rev. Lett.* 122, 250403. URL: <https://link.aps.org/doi/10.1103/PhysRevLett.122.250403>, doi:10.1103/PhysRevLett.122.250403.

- Bittel, L., Kliesch, M., 2021. Training variational quantum algorithms is np-hard. *Phys. Rev. Lett.* 127, 120502. URL: <https://link.aps.org/doi/10.1103/PhysRevLett.127.120502>, doi:10.1103/PhysRevLett.127.120502.
- Cabello, A., Severini, S., Winter, A., 2014. Graph-theoretic approach to quantum correlations. *Phys. Rev. Lett.* 112, 040401. URL: <https://link.aps.org/doi/10.1103/PhysRevLett.112.040401>, doi:10.1103/PhysRevLett.112.040401.
- Castaldo, D., Jahangiri, S., Delgado, A., Corni, S., 2022. Quantum simulation of molecules in solution. *Journal of Chemical Theory and Computation* 18, 7457–7469. URL: <https://doi.org/10.1021/acs.jctc.2c00974>, doi:10.1021/acs.jctc.2c00974, [arXiv:https://doi.org/10.1021/acs.jctc.2c00974](https://doi.org/10.1021/acs.jctc.2c00974). PMID: 36351289.
- Chen, J., Yang, T., Zhu, S., 2014. Efficient Low-Rank Stochastic Gradient Descent Methods for Solving Semidefinite Programs, in: Kaski, S., Corander, J. (Eds.), *Proceedings of the Seventeenth International Conference on Artificial Intelligence and Statistics*, PMLR, Reykjavik, Iceland. pp. 122–130. URL: <https://proceedings.mlr.press/v33/chen14b.html>.
- Eldar, Y., 2003. A semidefinite programming approach to optimal unambiguous discrimination of quantum states. *IEEE Transactions on Information Theory* 49, 446–456. doi:10.1109/TIT.2002.807291.
- Farhi, E., Goldstone, J., Gutmann, S., 2014. A quantum approximate optimization algorithm. [arXiv:1411.4028](https://arxiv.org/abs/1411.4028).
- Huang, H.Y., Bharti, K., Rebentrost, P., 2021. Near-term quantum algorithms for linear systems of equations with regression loss functions. *New Journal of Physics* 23, 113021.

- Lovász, L., Schrijver, A., 1991. Cones of matrices and set-functions and 0–1 optimization. *SIAM Journal on Optimization* 1, 166–190. URL: <https://doi.org/10.1137/0801013>, doi:10.1137/0801013, arXiv:<https://doi.org/10.1137/0801013>.
- Mazziotti, D.A., 2004. First-order semidefinite programming for the direct determination of two-electron reduced density matrices with application to many-electron atoms and molecules. *The Journal of chemical physics* 121, 10957–10966.
- McClean, J.R., Romero, J., Babbush, R., Aspuru-Guzik, A., 2016. The theory of variational hybrid quantum-classical algorithms. *New Journal of Physics* 18, 023023.
- Patel, D., Coles, P.J., Wilde, M.M., 2024. Variational quantum algorithms for semidefinite programming. [arXiv:2112.08859](https://arxiv.org/abs/2112.08859).
- Peruzzo, A., McClean, J., Shadbolt, P., Yung, M.H., Zhou, X.Q., Love, P.J., Aspuru-Guzik, A., O’Brien, J.L., 2014. A variational eigenvalue solver on a photonic quantum processor. *Nature Communications* 5, 4213. URL: <https://doi.org/10.1038/ncomms5213>, doi:10.1038/ncomms5213.
- Preskill, J., 2018. Quantum Computing in the NISQ era and beyond. *Quantum* 2, 79. URL: <https://doi.org/10.22331/q-2018-08-06-79>, doi:10.22331/q-2018-08-06-79.
- Schmidt, M.W., Baldridge, K.K., Boatz, J.A., Elbert, S.T., Gordon, M.S., Jensen, J.H., Koseki, S., Matsunaga, N., Nguyen, K.A., Su, S., et al., 1993. General atomic and molecular electronic structure system. *Journal of computational chemistry* 14, 1347–1363.

- Skrzypczyk, P., Šupić, I., Cavalcanti, D., 2019. All sets of incompatible measurements give an advantage in quantum state discrimination. *Phys. Rev. Lett.* 122, 130403. URL: <https://link.aps.org/doi/10.1103/PhysRevLett.122.130403>, doi:[10.1103/PhysRevLett.122.130403](https://doi.org/10.1103/PhysRevLett.122.130403).
- Wang, X., Xie, W., Duan, R., 2018. Semidefinite programming strong converse bounds for classical capacity. *IEEE Transactions on Information Theory* 64, 640–653. doi:[10.1109/TIT.2017.2741101](https://doi.org/10.1109/TIT.2017.2741101).